

# Development of SF<sub>6</sub>/O<sub>2</sub>/Si Plasma Etching Topography Simulation Model using New Flux Estimation Method

Tomoharu Ikeda, Hirokazu Saito,  
Fumiaki Kawai, Kimimori Hamada  
Electronics Development Div.3  
Toyota Motor Corporation, Aichi, Japan  
E-mail: t-ikeda@deco.tec.toyota.co.jp

Toshimitsu Ohmine, Hideki Takada,  
Silicon Engineering Group  
Nihon Synopsys G.K., Tokyo, Japan

Vaibhav Deshpande  
Silicon Engineering Group  
Synopsys Switzerland LLC., Zurich, Switzerland

**Abstract-** A new topography simulation method has been developed for SF<sub>6</sub>/O<sub>2</sub>/Si plasma etching of trench gates in IGBTs. This method calculates the ion and fluorine radical flux parameters required for the topography simulation from the etching rate and selectivity obtained from simple basic experiments. The O radical flux was assumed as a function of the operating conditions and the function form was determined by fitting etching profiles of the topography simulation to those of the experiment. The model used in the topography simulation was improved in terms of the etching yield dependence on the ion incidence angle. As a result, a large variety of profiles could be simulated accurately under different operational conditions.

**Keywords-** ion; fluorine; flux; etching; ion-enhanced; SF<sub>6</sub>; selectivity; topography; simulation; yield; silicon

## I. INTRODUCTION

Hybrid vehicles (HVs) and electric vehicles (EVs) have higher fuel efficiency and lower CO<sub>2</sub>/NO<sub>x</sub> emissions than conventional vehicles. Further technical development of these vehicles is urgently required to help resolve environmental problems such as global warming. Insulated gate bipolar transistors (IGBTs) are a key component in these vehicles for switching high currents, and play a critical role in determining fuel efficiency. The performance of IGBTs has been greatly enhanced by the adoption of a trench gate structure [1]. However, severe controls have to be applied to the profile of the trench to improve performance and to secure the required quality. For this reason, it is important to develop a method that does not rely on trial and error.

This paper describes the development of trench etching topography simulation methodology for SF<sub>6</sub>/O<sub>2</sub>/Si ion-assisted etching, in which the ion/radical flux is simulated based on the mask-to-body selectivity and the etching rate. It also describes how the topography simulation accuracy was improved under a wide range of operational conditions, mainly by optimizing the etching yield curve and the function form of the O radical flux that is dependant on the operating conditions.

## II. METHOD AND THEORY

### Development of flux estimation method

Equations were derived based on the literature, correlating the ion and fluorine (F) flux with the etching rate and mask selectivity, which can be readily obtained through basic experiments using a production etching machine [2].

In the etching of Si with SF<sub>6</sub> and O<sub>2</sub> gases with a SiO<sub>2</sub> mask, SiO<sub>2</sub> etching is virtually regarded as an ion governing process since the surface is saturated with adsorbed F radicals making the surface coverage a constant value of unity [3]. In contrast, Si etching is greatly affected by the F concentration, and it can be considered that Si/SiO<sub>2</sub> etching selectivity reflects this difference. Based on a successful modeling study [4], Equation (1) can be derived for ion flux as a function of the Si etching rate and selectivity, by regarding the SiO<sub>2</sub> etching as a pure ion governing process.

$$\Gamma_i = \frac{\rho_{SiO_2}}{Y_{SiO_2}} \frac{Er_{Si}}{S} \quad (1)$$

where,  $\rho_{SiO_2}$  is the SiO<sub>2</sub> molecular density,  $Er_{Si}$  is the Si etching rate obtained from experiments,  $Y_{SiO_2}$  is the SiO<sub>2</sub> etching yield, and  $S$  is the Si/SiO<sub>2</sub> etching selectivity obtained from experiments.

The F radical flux  $\Gamma_F$  is described as follow considering that the Si etching rate is affected by O on the Si surface.

$$\Gamma_F = \frac{1}{\gamma_F} \frac{\theta_F}{(1-\theta_F)} (k_{Si} + 2Y_{Si}\Gamma_i) \left(1 + \frac{\gamma_O\Gamma_O}{Y_O\Gamma_i}\right) \quad (2)$$

where,  $\gamma_F$  and  $\gamma_O$  are the sticking coefficients for F and O radicals respectively,  $\theta_F$  is the surface coverage of F,  $k_{Si}$  is the spontaneous reaction speed of Si and F,  $\Gamma_O$  is the O radical flux, and  $Y_F$  and  $Y_O$  is the etching yield of the F and O radicals adsorbed on the Si surface.

$\theta_F$  can be obtained in the following equation, where  $\rho_{Si}$  is the Si molecular density and  $Y_{Si}$  is the yield of the Si ion-assisted reaction.

$$\theta_F = \frac{\rho_{Si} Y_{SiO_2}}{\rho_{SiO_2} Y_{Si}} S \quad (3)$$

#### Estimation of O radical flux

Equation (2) requires the O radical flux to calculate the F radical flux. The dependence on the operating conditions was estimated using the following equation and the indices in the equation were optimized based on the consistency of the etching topography.

$$\Gamma_O = A \times P^l \times F_O^m \times W^n \quad (4)$$

where,  $A$  is the proportionality constant,  $P$  is the chamber pressure,  $F_O$  is the O<sub>2</sub> flow rate, and  $W$  is the RF power input value. According to plasma simulation results and the results of past experiments [4], the F:O radical ratio is assumed as approximately 20:1.

#### Experiment

The experiment used a magnetron capacitively coupled plasma (CCP) etching machine with an excitation frequency of 40.7 MHz to perform SiO<sub>2</sub> hard mask Si trench etching. The etching rate and selectivity were measured from cross section views of SEM images. The operating conditions were varied within the following ranges: pressure = 120 to 220 mTorr, input power = 1,200 to 2,000 W, and O<sub>2</sub> flow rate ratio to total flow rate = 30 to 40%. The electrode gap was varied between 27 and 47 mm.

#### Topography simulator and reaction model

The trench topography simulation is capable of handling the surface reactions kinetically. The simulator uses a radiosity matrix to calculate the flux and the level set method to calculate the feature evolution [5]. The surface reaction model that was used is as follows.

1.  $F + Si \rightarrow SiF$
2.  $SiF + 3F \rightarrow SiF_4 \uparrow$
3.  $SF_3^+ + SiF + F \rightarrow SiF_2 \uparrow$
4.  $O + Si \rightarrow SiO$
5.  $SiO \rightarrow 1/2 O_2 + Si$
6.  $SF_3 + SiO \rightarrow SF_3 + O \uparrow + Si$

Each reaction rate coefficient was adopted from a previous study [4] using the same gas and materials (Table 1).

TABLE 1. PARAMETER VALUES USED IN TOPOGRAPHY SIMULATION

Constants used	Value
$k_{Si}$ (mol/m <sup>2</sup> /s)	0.005
$Y_{Si}$	7.0
$Y_{SiO}$	3.0
$\gamma_F$	0.7
$\gamma_O$	1.0

The function of etching yield change with respect to the ion incidence angle has a major effect on etching topography. Belen and et al. [6] obtained different yield curve results (Fig. 1) when the etching was performed with pure SF<sub>6</sub> gas (i.e., without O<sub>2</sub> gas) and with a blended gas consisting of both SF<sub>6</sub> and O<sub>2</sub>. In the present research, we approximated the two curves with the following functions.

a) Without O<sub>2</sub>

$$1 - \{\sin(\theta)\}^{21} \quad (5)$$

b) With O<sub>2</sub>

$$\frac{\{0.01 - \sin(0.3 \times \theta)\}^5}{0.01} \quad (6)$$

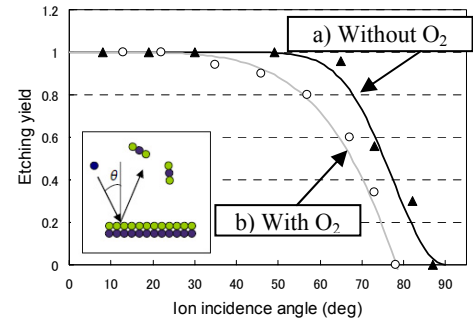


Fig. 1 Angle dependence of the Si etching yield in SF<sub>6</sub>/O<sub>2</sub> plasma

We tried curve b) for the reaction eq. 6 and curves between a) and b) for the reaction eq. 3.

### III. RESULTS

The Si etching rate and SiO<sub>2</sub> selectivity obtained in the experiment were substituted into eq. (1) to calculate the ion flux  $\Gamma_i$ . The F flux  $\Gamma_F$  was calculated from eq. (2). The O flux  $\Gamma_O$  was calculated by substituting the experiment control parameters with the indices in eq. (4) all set to 1 as initial values. The topography simulation was then performed using each calculated flux as input.

#### Correction of ion flux

Comparing the simulation and experiment results for the Si etching rate (hereafter “average etching rate”) calculated from the time to achieve a trench depth of 5 μm, the simulation gave a lower etching rate under all experimental conditions. This is because the average etching rate of the experiment was used in the flux calculation. The flux for the topography simulation should be calculated from the initial etching rate, not the average, which has a minimal shadowing effect and diffusion resistance.

However, in high aspect ratio etching, the etching rate is not constant, decreasing with the trench depth, as shown in Fig. 2, resulting in an average etching rate that is lower than the initial rate [7].

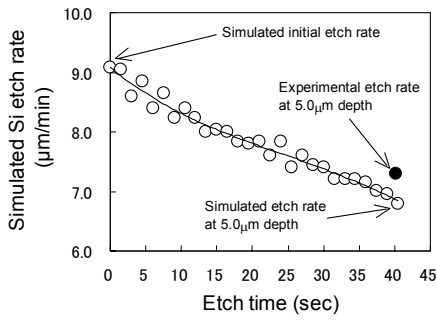


Fig.2 Example of time-dependent variation of etching rate

For this reason, the following procedure was carried out to estimate the initial etching rate.

- 1) Using an experimentally obtained average etching rate, calculate an ion flux and F radical flux.
- 2) Using the flux values obtained in step 1), carry out topography simulation
- 3) From the time-dependent etching rate curve obtained in step 2), take the ratio of the simulated average etching rate to that of the experiment, which is multiplied by the simulated initial etching rate to obtain a new initial etching rate.
- 4) Using the new initial etching rate and selectivity, recalculate fluxes.

Using the corrected values for the fluxes, the average Si etching rate was found to closely match the rate in experiment (Fig. 3).

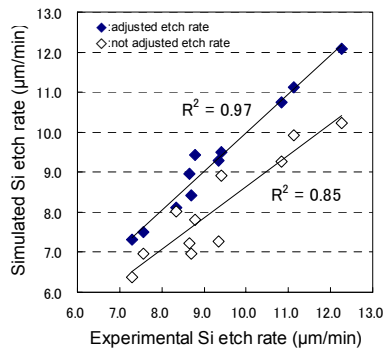


Fig.3 Comparison of simulated etch rates against experimental etch rates

### Optimization of O flux function

In the etching topography simulation, using the ion and F flux values calculated as described above and the O flux value calculated with the exponents in eq. (4) all set to 1, the etching profiles were not sensitive enough for visual comparison to the changes in the exponents in the eq. (4).

Therefore, the comparison was made by measuring the trench width 1 µm above the bottom between the experiment and the simulation. Using the R square correlation of the trench widths (Figs. 4 and 5), the optimum O flux function is obtained as follows.

$$\Gamma_o = A \times P^{0.5} \times F_o^2 \times W^{0.2} \quad (4)'$$

The strong correlation to the O flow rate in the above equation is the same as that found in reference [3].

### Study of etching yield curve

In the simulation using yield curve a) for reaction eq. 3 and curve b) for reaction eq. 6, the obtained topography did not closely reproduce the strong taper (the profile with a small trench bottom width) when the F radical flux/ion flux ratio was large. Case A and B in Fig. 6 compares the simulation results with a different F/ion flux ratio; a smaller ratio for case A than case B. Using the yield curves a) and b) for reaction eqs. 3 and 6 respectively in the simulation, case A has a stronger taper than B, while in the SEM image, the reverse is true.

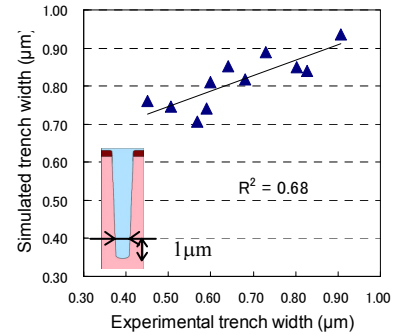


Fig.4 Comparison of simulated trench width against experimental trench width (input values: l=1, m=1, n=1)

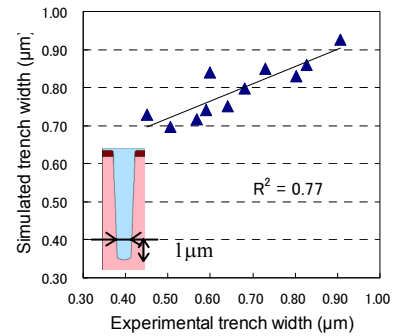


Fig.5 Comparison of simulated trench width against experimental trench width (input values: l=0.5, m=2, n=0.2)

In yield curve a) in the Fig.1, the etching reaction continues until the ion incidence angle is almost 90°. This causes the etching reaction to proceed laterally to the trench walls, making it difficult to obtain a strong trench taper.

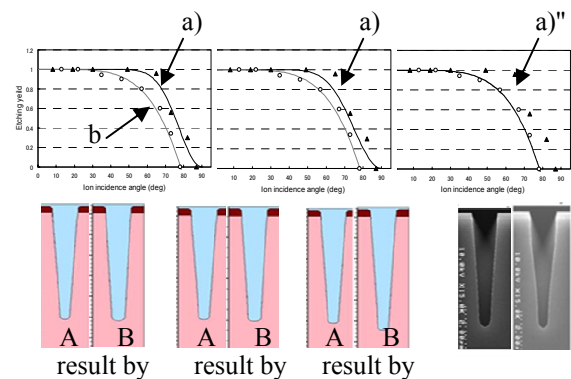


Fig. 6 Etching profile change according to variation in etching yield curve

As shown in Fig.6, it was found that moving yield curve a) for reaction eq. 3 closer to curve b), the taper angle under condition B becomes smaller and a better agreement with the experiment (SEM cross sectional view in Fig.6) is obtained.

Figure 7 compares an example of the optimized topography simulation results with the experiment results. The simulation results are consistent with the experiment over a wide range of operating conditions. The trench width correlation was improved from  $R^2=0.77$  to 0.83 (Fig. 8).

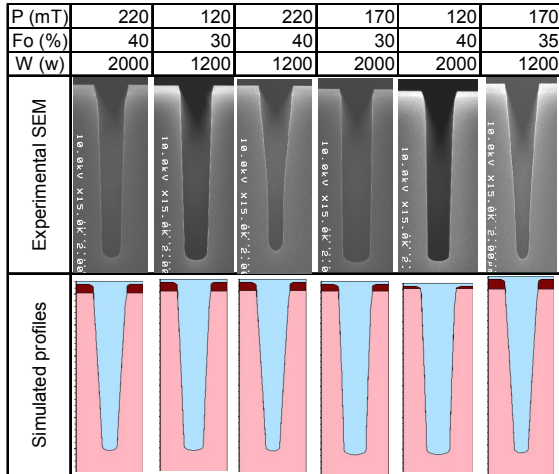


Fig.7 Simulated etching profiles compared with experimental SEM profiles

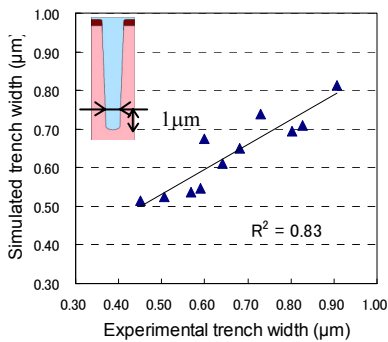


Fig.8 Comparison of simulated trench width against experimental trench width

*Example of flux calculation and simulation results*

Figure 9 shows a spatial distribution of the F radical and ion flux calculated by the developed method, and the comparison of simulated profiles against experimental profiles at various position of wafer (0 = wafer center).

It shows that the distribution of the ion flux is higher at the center of the wafer and that the radical flux is higher at the edges. This result is qualitatively consistent with the results of the plasma simulation [8]. The etching profile trend with a wider trench at the center and narrower toward the edge, is well reproduced by the simulation using corresponding flux values as input.

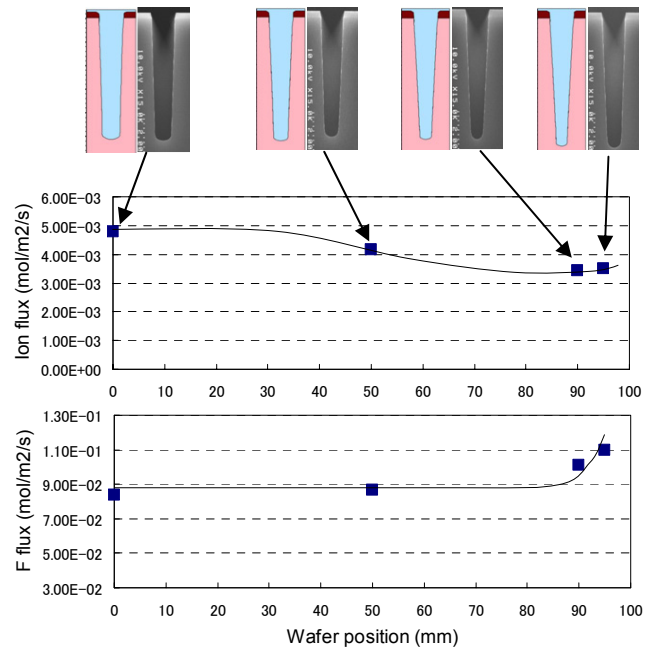


Fig.9 Ion and F flux profile across a wafer with corresponding etching profile.

IV. CONCLUSION

A calculation method for ion and F radical flux was developed based on the measured etching rates and mask-body selectivity obtained in experiments which were performed using an SF<sub>6</sub>/O<sub>2</sub>/Si plasma etching production machine. The fluxes thus obtained showed qualitatively reasonable trend. Using the obtained fluxes and by optimizing the O radical flux calculation equation and etching yield curve, simulated trench profiles proved to reproduce those of experiments for a wide range of operating conditions.

REFERENCES

- [1] K. Hamada, T. Kushida, A. Kawahashi, and M. Ishiko, Proceedings of ISPSD'01, pp.449-452 (2001)
- [2] T. Ohmine, V. Deshpande, H. Takada, T. Ikeda, H. Saito, F. Kawai, and K. Hamada: to be published in Jpn. J. Appl. Phys., Aug. (2011)
- [3] A. Mahorowala, H. Sawin: J. Vac. Sci. Technol. B20(3) 1064(2002)
- [4] R. Belen, S. Gomez, D. Cooperberg, M. Kiehlbauch, and E. Aydil: J. Vac. Sci. Technology. A 23(5), 1430 – 1439(2005)
- [5] Synopsys, Inc (2009). Sentaurus Topography User Guide
- [6] R. Belen, S. Gomez, M. Kiehlbauch, and E. Aydil: J. Vac. Sci. Technol. A24(6), 2176 (2006)
- [7] I. Sakai, N. Sakurai, and T. Ohiwa: Proceedings of DPS'08, pp125-126 (2008)
- [8] Esgee Technologies, Inc. (2009). VizGlow User Guide